A symmetrical ionic liquid/Li salt system for rapid ion transport and stable lithium electrochemistry

Journal:	*ChemComm*
Manuscript ID	CC-COM-01-2018-000531.R2
Article Type:	Communication

ChemComm

COMMUNICATION

A symmetrical ionic liquid/Li salt system for rapid ion transport and stable lithium electrochemistry

Danah Al-Masri,[a] Ruhamah Yunis,[a] Anthony F. Hollenkamp[b] and Jennifer M. Pringle[a]

Received 00th January 20xx,
Accepted 00th January 20xx

DOI: 10.1039/x0xx00000x

www.rsc.org/

Contrary to the accepted wisdom that avoids cation symmetry for the sake of optimum electrolyte properties, we reveal outstanding behaviour for the diethylpyrrolidinium cation ([C_2epyr]), in combination with the bis(fluorosulfonyl)imide (FSI) anion and Li[FSI]. The equimolar [C_2epyr][Li][FSI]$_2$ is a liquid with high conductivity, high Li transference number and > 90% lithium metal cycling efficiency. The high level of performance for these electrolytes invites consideration of a new class of electrolytes for lithium batteries.

The rapidly increasing use of portable electronics, electric vehicles and so forth has created an urgent need for safer batteries with high capacity and rate capabilities. One of the associated challenges is to develop electrolytes that can enable the development of electrochemical energy storage technologies beyond the present lithium-ion batteries, such as those utilising lithium metal. The negligible volatility and flammability and wide electrochemical window of many ionic liquids (ILs) is highly beneficial for their use in batteries,[1-3] and the efficient cycling of lithium metal in ILs has been well demonstrated.[4-6] The main advantage of using IL-based electrolytes in lithium batteries is the enhanced safety that is provided by the negligible vapour pressure. Standard lithium battery electrolytes are based on organic carbonates and, even though these have a relatively high boiling point, any fault that causes heating of a cell/battery will still lead to increased internal gas pressure which, ultimately, will end up in the venting of flammable vapour and subsequent fire or explosion. With no volatile component, IL-based electrolytes are safe in this regard. The *N*-alkyl-*N*-methylpyrrolidinium cation ([$C_n$mpyr]$^+$) has proven exceptionally useful for the development of ILs with high fluidity and electrochemical stability. In battery applications, the [$C_n$mpyr]$^+$ cation is most commonly paired with either the bis(trifluoromethylsulfonyl)imide (NTf_2) or bis(fluorosulfonyl)imide (FSI) anion, the latter of which generally exhibits the most promising electrochemical performance.[4, 5, 8, 9] However, the widespread use of IL-based electrolytes is still largely hindered by the relatively poor target ion (e.g. Li$^+$) transport, compared to that in traditional, more fluid organic solvent systems, which limits the battery rate capability. Thus, there exists a continued need to develop new electrolytes with enhanced transport, in combination with sufficient electrochemical stability and safety.

We have recently demonstrated that use of the symmetrical *N,N*-diethylpyrrolidinium cation ([C_2epyr]$^+$), instead of the methyl-substituted analogue, can produce a range of solid and liquid electrolytes with advantageous thermal and transport properties.[10] In that first exploration of the new electrolyte family, pairing the [C_2epyr]$^+$ cation with the fluorosulfonyl(trifluoromethanesulfonyl)imide ([FTFSI]$^-$) or dicyanamide ([DCA]$^-$) anions produced room temperature ILs with low viscosity. With the bis(trifluoromethylsulfonyl)imide ([NTf_2]$^-$), bis(fluorosulfonyl)imide ([FSI]$^-$), hexafluorophosphate ([PF_6]$^-$) or tetrafluoroborate ([BF_4]$^-$) anions, organic ionic plastic crystals (OIPCs) were produced. OIPCs are a specific type of salt structurally analogous to ILs but solid at room temperature and with significant disorder within the crystal lattice. These materials have recently shown significant promise as solid-state electrolytes, for example when combined with Li or Na salts for use in Li or Na batteries, and again the FSI anion is proving to be particularly beneficial with respect to achieving high conductivities and electrochemical performance.[12-16] Of the new OIPCs, [C_2epyr][FSI] had the highest conductivity, giving 1.9×10^{-5} S cm^{-1} at 30 °C.[10]

An emerging new direction for battery electrolyte research is the exploration of high concentration electrolytes, for use in Li or Na batteries.[17-19] In such systems, the Li or Na salt that is required for battery operation is dissolved in the solvent or IL at

---

[a] Deakin University, Melbourne, Institute for Frontier Materials, Victoria 3125, Australia. Email:jenny.pringle@deakin.edu.au.

[b] Commonwealth Scientific and Industrial Research Organisation (CSIRO), Clayton, 3168, VIC, Australia.

† Electronic Supplementary Information (ESI) available: Synthetic and analytical procedures. See DOI: 10.1039/x0xx00000x

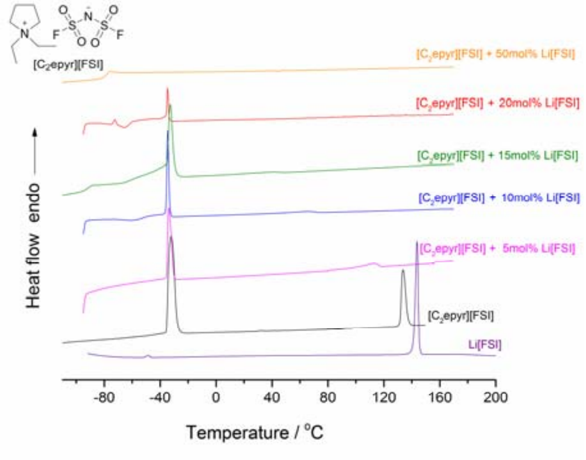

Figure 1. The DSC traces of [C$_2$epyr][FSI] with increasing concentration of Li[FSI]. Inset: the structure of [C$_2$epyr][FSI].

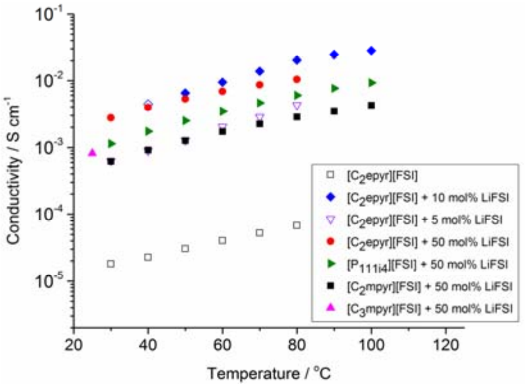

Figure 2. The conductivity of [C$_2$epyr][FSI] containing different molar concentrations of Li[FSI]. The conductivity of [C$_2$mpyr][FSI],[7] [C$_3$mpyr][FSI],[6] and [P$_{111i4}$][FSI],[11] systems with 50 mol% Li[FSI] are shown for comparison. Solid symbols - material was liquid at the temperature of measurement; open symbols - material was solid, or had some solid phase, at the temperature of measurement.

concentrations of > 1M, in some cases over 50 mol%. The higher concentration of target ion offers the possibility of higher transference number and better battery cycling performance through improved interfacial reactions. Higher transference number translates directly to higher charging and discharging currents in a given battery. This means that the device will operate at greater Coulombic efficiency under a given set of conditions. Better cycling performance (i.e., the ability to complete more charge-discharge cycles prior to the discharge capacity reaching an agreed end-point (usually 80% of initial capacity) is the key parameter when determining the lifetime cost of a battery as the true cost of a battery is really measured either per completed cycle, or per unit of charge throughput. For lithium batteries, the concept of high salt content has been demonstrated in organic solvent-based systems.[8, 20] More recently, in the IL field this has led to new “inorganic-organic ionic liquid”, “binary” or “super-concentrated” systems. This concept has recently has been utilised in FSI-based ILs with either a phosphonium cation (termed [P$_{111i4}$], where the number indicates the length of the alkyl chain and i4 indicates *iso*-butyl)[21] or an *N*-methyl-*N*-alkyl pyrrolidinium cation.[5, 6] For example, Paillard *et al.*[5] studied the effect of Li[FSI] concentration in [C$_4$mpyr][FSI], up to a mole fraction of 0.4. At this higher concentration, the material is amorphous and supports efficient lithium cycling. The [C$_2$mpyr][FSI] OIPC has also been combined with Li[FSI] and electrospun polyvinylidene fluoride (PVDF) nanofibers to make high concentration composite membranes that support good lithium metal battery performance.[7]

Here we report the synthesis and characterisation of a new super-concentrated electrolyte, [C$_2$epyr][Li][FSI]$_2$. Using a high conductivity OIPC as a starting point, by utilising the diethylpyrrolidinium cation in combination with the FSI anion, addition of an equimolar amount of Li[FSI] allows access to high conductivities and a high lithium transference number.

The [C$_2$epyr][FSI] can be synthesised by the direct reaction of *N*-ethylpyrrolidine with ethylbromide to form [C$_2$epyr]Br, followed by metathesis with K[FSI]. Full synthetic details are given in the Supporting Information. The [C$_2$epyr][FSI] is a soft solid at room temperature. This can be combined with specific quantities of Li[FSI] by mixing the two salts in dry acetonitrile, followed by rigorous drying under vacuum. At room temperature, the [C$_2$epyr][FSI] is an organic ionic plastic crystal (OIPC);[22, 23] it undergoes a large-entropy-change solid-solid phase transition at -35 °C and then melts at 131 °C (Figure 1). This salt also has a relatively low entropy of melt, at only 9 J K^{-1} mol^{-1}, which is typical of plastic crystals as it reflects the significant disorder that exists in the plastic phase.[24]

Figure 1 shows the change in thermal properties of [C$_2$epyr][FSI] with increasing concentrations of Li[FSI]. Upon addition of a small amount (5-10 mol%) of Li[FSI], the melt transition moves to lower temperatures and becomes broader. This is consistent with the effect of alkali metal salt addition to other OIPCs,[5, 12, 16, 25] where the salt acts as an “impurity” and thus broadens and lowers the melt transition. With 10 mol% Li[FSI], at room temperature the material visually appears to be composed of both solid and liquid phases. The melting transition of the solid component is small and very broad, with an onset of approximately 50 °C. At this composition, there is also a subtle exothermic peak at ca. -60 ^{o}C, which may indicate the crystallisation of a eutectic phase, with the eutectic melt overlapping with the solid-solid transition at ca. -34 °C. Attempts to separate these two endothermic events by running at the DSC at a lower scan rate (1 °C/min) were not successful. The ΔS of the low temperature endothermic transition decreases with increasing Li[FSI] content (Table 1), consistent with the decreasing amount of [C$_2$epyr][FSI]. The sample with 15 mol % Li[FSI] shows more clearly the presence of an additional endothermic phase transition, at ca. -50 °C, before the larger transition at -34 °C (this shoulder is not included in the entropy value given in Table 1). The low temperature exothermic transition, tentatively attributed to a eutectic composition, is more pronounced with 20 mol % Li[FSI]. The formation of a eutectic composition at low alkali salt content has also been observed in other FSI systems, such as the K[FSI]/[C$_3$mpyr][FSI],[26] and Na[FSI]/[P$_{1i444}$][FSI].[12]

At concentrations of ≥ 20 mol% Li[FSI] in [C_2epyr][FSI], the material is entirely liquid at room temperature. This indicates either that the melting point was reduced to below room temperature or that the liquid is in a supercooled, metastable state. However, we have seen no evidence of crystallisation of this material after months of study. At higher salt concentrations (≥ 70 mol% Li[FSI]), a second, solid phase is visible at room temperature. Thus, for the purposes of developing a high concentration liquid electrolyte with optimum lithium transport properties, the sample with 50 mol% Li[FSI] (≡ 3.2 mol kg^{-1}) was chosen for further study. At this composition, which can also be represented as [C_2epyr][Li][FSI]$_2$, the material is a colourless glass-forming liquid that displays only a T_g at -75 °C.

Table 1. Transition temperatures (onset) and entropies for the [C_2epyr][FSI] / Li[FSI] salts. T_g = glass transition, T_s = solid-solid transition, T_m = melting. *At 5-20% Li[FSI], this endothermic transition may also overlap with the melting of a eutectic phase.

	T_g / °C ± 1	T_s* / °C ± 1	ΔS / J K^{-1} mol^{-1} ± 1	T_m / °C ± 1	ΔS / J K^{-1} mol^{-1} ± 1
[C_2epyr][FSI]	-	-35	36	131	9
[C_2epyr][FSI] +5%mol Li[FSI]	-	-34	26	98	2
[C_2epyr][FSI]+10 mol% Li[FSI]	-	-34	16	~ 50	~ 1
[C_2epyr][FSI]+15 mol% Li[FSI]	-	-34	8	-	-
[C_2epyr][FSI]+20 mol% Li[FSI]	-72	-34	5	-	-
[C_2epyr][FSI]+50 mol% Li[FSI]	-75	-	-	-	-
Li[FSI]	-	-51	2	140	41

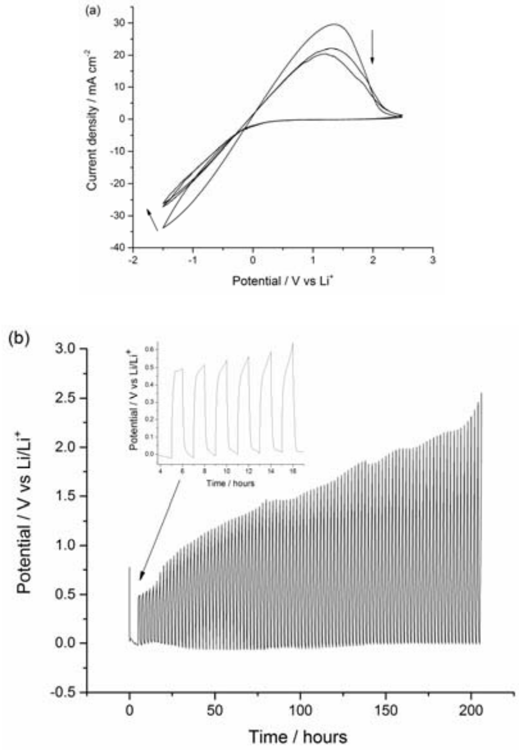

Figure 3. (a) The cyclic voltammogram of [C_2epyr][Li][FSI]$_2$ at room temperature - the arrows show the direction of peak progression from the 1st to the 3rd scan, (b) cycling of the [C_2epyr][Li][FSI]$_2$ over 100 cycles at a current density of 0.5mA.cm^{-2}. With platinum working electrode (2.0 mm^2 surface area), a lithium strip as a quasi-reference electrode and a coiled lithium metal strip as counter electrode.

The ionic conductivities of the neat OIPC and with different concentrations of Li[FSI] are shown in Figure 2. For comparison, the conductivity of analogous [C_2mpyr][FSI], [C_3mpyr][FSI] and [P_{111i4}][FSI] systems with 50 mol% Li[FSI] are also given, all of which lie below the new [C_2epyr][Li][FSI]$_2$. One of the challenges of increasing the concentration of Li salt in an ionic liquid is that this commonly results in an increase in viscosity and, thus, a decrease in conductivity. However, as introduced above, the recent reports of high concentration salt systems demonstrate that the optimum salt concentration for target ion transport can be very high.[17, 18, 20] In the [C_2epyr][FSI]-based electrolytes, the sample with 10 mol% Li[FSI], which is predominantly a liquid, with some solid present until > ca. 50 °C , has the highest conductivity, markedly higher than that for the neat [C_2epyr][FSI] (Figure 2). Increasing the concentration of Li[FSI] to 50 mol% results in only a minor decrease in conductivity compared to the 10 mol% system, giving a conductivity of 2.7 mS cm^{-1} at 30 °C. This is appreciably more conductive than the 50 mol% Li[FSI] in [C_3mpyr][FSI] (0.82 mS cm^{-1} at 25 °C),[6] the 50 mol% Li[FSI] in [C_2mpyr][FSI] (0.63 mS cm^{-1} at 30 °C),[7] or 50 mol% Li[FSI] in [P_{111i4}][FSI] (1.14 mS cm^{-1} at 30 °C)[11] electrolytes reported previously. Paillard *et al.*[5] reported a conductivity of 3.7 mS cm^{-1} at 25 °C for [C_4mpyr][FSI] containing 0.1 mole fraction of Li[FSI] but this decreases significantly upon addition of more Li[FSI], consistent with a significant increase in viscosity (exact numbers not given).

The trend in conductivity with change in IL cation (all with 50 mol% Li[FSI]) is not entirely explained by the viscosity. The viscosity of [C_2epyr][Li][FSI]$_2$ is 302 mPa.s at 25 °C. The viscosity of the [P_{111i4}][FSI] with 50 mol% Li[FSI] is 323 ± 10 mPa s,[11] consistent with the lower conductivity. However, the reported viscosity of [C_3mpyr][FSI] with 50 mol% Li[FSI] is only 253 mPa.s at 25 °C,[6] and thus the lower conductivity (and much lower Li transference number, discussed below) suggests differences in speciation compared to [C_2epyr][Li][FSI]$_2$.

One of the key requirements for an efficient electrolyte for lithium batteries, to support high cycling rates, is that the fraction of charge carried by the target ion is as high as possible. High lithium transference number, t_{Li^+}, has recently emerged as one of the benefits of high concentration inorganic-organic ionic liquids; the general trend is such that increasing the Li concentration increases the transference number.[6, 17] Here, the t_{Li^+} of the [C_2epyr][Li][FSI]$_2$ was measured within a symmetrical lithium coin cell at 50 °C,[27] and determined to be 0.39 ± 0.03. This compares well to t_{Li^+} measured previously in systems with 50 mol% Li[FSI]: 0.183 ± 0.008 in [C_3mpyr][FSI] (25 °C),[6] 0.46 ± 0.04 in [P_{111i4}][FSI] (25 °C),[17] and 0.37 ± 0.02 (50 °C) in

[C_2mpyr][FSI] within a PVDF membrane.[7] It is also significantly higher than the 0.13 reported for a 0.32 mol.kg^{-1} Li[NTf_2] in *N*,*N*-diethyl-*N*-methyl-*N*-2-methoxyethylammonium NTf_2 (60 °C),[19] and equivalent to the 0.39 achieved at 0.7 mole fraction of Li[NTf_2] in *N*-methoxyethyl-*N*-methylpyrrolidinium NTf_2.[28]

High efficiency of lithium metal deposition and stripping is critical in supporting the cycling performance of lithium metal batteries. The solid electrolyte interphase (SEI)[29] must be stable and able to support high lithium-ion conductivity. This was assessed here by means of cyclic voltammetry (CV) analysis in a three-electrode cell.[30] The voltammograms of [C_2epyr][Li][FSI]$_2$ (Figure 3a) show well-defined deposition and stripping processes for Li during repetitive potential-cycling at room temperature. Estimates of Coulombic efficiency were over 80% for the first two cycles, decreasing to 71% for the third cycle. The oxidative and reductive current densities also decrease slightly with cycling, consistent with the progressive formation of an SEI layer on the lithium metal surface.

To obtain a more accurate measure of the reversibility of lithium deposition-stripping, galvanostatic cycling of a known amount of lithium is usually undertaken. Here, a pre-deposited quantity of lithium was cycled in the [C_2epyr][Li][FSI]$_2$ electrolyte using the same three-electrode cell setup at a controlled current density of 0.5 mA.cm^{-2}, and 0.5 mA.h.cm^{-2} of charge passed in each step (Figure 3b). The inset shows an expanded view of the first six cycles, where the potential increase is consistent with the behaviour of other IL/salt systems.[30] Under these conditions, an increase in potential is a characteristic of the build-up of a more resistive SEI layer and “dead lithium” on the Li surface. Ultimately, these processes limit the cycle-life that can be achieved in all electrolyte systems. Here the rate of increase of potential and the value eventually reached are modest, such that [C_2epyr][Li][FSI]$_2$ permits efficient cycling, with an average efficiency of 96%, for 100 cycles, after which time the experiment was stopped. The maximum potential measured after 100 cycles was 2.55 V vs Li/Li$^+$, which is well within the electrochemical window of stability of the electrolyte, measured to be >3.6 V (Figure S1). This initial cycling response indicates good stability of the Li surface in this electrolyte, i.e. the formation of a relatively stable and conductive SEI layer and no rapid build-up of inactive Li deposits. In summary, this stable electrochemical behaviour, in addition to the high lithium transference number, strongly supports the further investigation of [C_2epyr][Li][FSI]$_2$ for use as an electrolyte material in lithium metal batteries. Moreover, other symmetrical cations may now be considered for application in this continually growing area of research.

This work was supported by the Australian Research Council through Discovery Grant DP170101087.

Conflicts of interest

There are no conflicts to declare.

Notes and references

[1]. M. Armand, F. Endres, D. R. MacFarlane, H. Ohno, B. Scrosati, *Nat. Mater.*, 2009, **8**, 621.

[2]. M. Watanabe, M. L. Thomas, S. Zhang, K. Ueno, T. Yasuda, K. Dokko, *Chem. Rev.*, 2017, **117**, 7190.

[3]. D. R. MacFarlane, M. Forsyth, P. C. Howlett, M. Kar, S. Passerini, J. M. Pringle, H. Ohno, M. Watanabe, F. Yan, W. Zheng, S. Zhang, J. Zhang, *Nat. Rev.*, 2016, **1**, 15005.

[4]. A. S. Best, A. I. Bhatt, A. F. Hollenkamp, *J. Electrochem. Soc.*, 2010, **157**, A903.

[5]. E. Paillard, Q. Zhou, W. A. Henderson, G. B. Appetecchi, M. Montanino, S. Passerini, *J. Electrochem. Soc.*, 2009, **156**, A891.

[6]. H. Yoon, P. C. Howlett, A. S. Best, M. Forsyth, D. R. MacFarlane, *J. Electrochem. Soc.*, 2013, **160**, A1629.

[7]. Y. Zhou, X. Wang, H. Zhu, M. Yoshizawa-Fujita, Y. Miyachi, M. Armand, M. Forsyth, G. W. Greene, J. M. Pringle, P. C. Howlett, *ChemSusChem*, 2017, **10**, 3135.

[8]. J. Qian, W. A. Henderson, W. Xu, P. Bhattacharya, M. Engelhard, O. Borodin, J.-G. Zhang, *Nat. Commun.*, 2015, **6**, 6362.

[9]. Q. Zhou, W. A. Henderson, G. B. Appetecchi, M. Montanino, S. Passerini, *J. Phys. Chem. B*, 2008, **112**, 13577.

[10]. R. Yunis, T. W. Newbegin, A. F. Hollenkamp, J. M. Pringle, *Materials Chemistry Frontiers*, 2018, Submitted.

[11]. G. M. A. Girard, M. Hilder, H. Zhu, D. Nucciarone, K. Whitbread, S. Zavorine, M. Moser, M. Forsyth, D. R. MacFarlane, P. C. Howlett, *PCCP.*, 2015, **17**, 8706.

[12]. F. Makhlooghiazad, P. C. Howlett, X. Wang, M. Hilder, D. R. MacFarlane, M. Armand, M. Forsyth, *J. Mat. Chem. A*, 2017, **5**, 5770.

[13]. J. M. Pringle, *PCCP.*, 2013, **15**, 1339.

[14]. Y. Shekibi, T. Ruether, J. Huang, A. F. Hollenkamp, *PCCP.*, 2012, **14**, 4597.

[15]. M. Yoshizawa-Fujita, E. Kishi, M. Suematsu, T. Takekawa, M. Rikukawa, *Chem. Lett.*, 2014, **43**, 1909.

[16]. L. Jin, P. C. Howlett, J. M. Pringle, J. Janikowski, M. Armand, D. R. MacFarlane, M. Forsyth, *Energy & Env. Sci.*, 2014, **7**, 3352.

[17]. M. Forsyth, G. M. A. Girard, A. Basile, M. Hilder, D. R. MacFarlane, F. Chen, P. C. Howlett, *Electrochim. Acta*, 2016, **220**, 609.

[18]. Y. Yamada, A. Yamada, *J. Electrochem. Soc.*, 2015, **162**, A2406.

[19]. S. Seki, Y. Ohno, H. Miyashiro, Y. Kobayashi, A. Usami, Y. Mita, N. Terada, K. Hayamizu, S. Tsuzuki, M. Watanabe, *J. Electrochem. Soc.*, 2008, **155**, A421.

[20]. L. Suo, Y.-S. Hu, H. Li, M. Armand, L. Chen, *Nat. Commun.*, 2013, **4**, 1481.

[21]. G. M. A. Girard, M. Hilder, D. Nucciarone, K. Whitbread, S. Zavorine, M. Moser, M. Forsyth, D. R. MacFarlane, P. C. Howlett, *J. Phys. Chem. C*, 2017, **121**, 21087.

[22]. D. R.MacFarlane, J. Huang, M. Forsyth, *Nature*, 1999, **402**, 792.

[23]. D. R. MacFarlane, P. Meakin, N. Amini, M. Forsyth, *J. Phys.: Condens. Matter*, 2001, **13**, 8257.

[24]. J. Timmermans, *J. Phys. Chem. Solids*, 1961, **18**, 1.

[25]. W. A. Henderson, D. M. Seo, Q. Zhou, P. D. Boyle, J.-H. Shin, H. C. De Long, P. C. Trulove, S. Passerini, *Adv. Energy Mater.*, 2012, **2**, 1343.

[26]. T. Yamamoto, K. Matsumoto, R. Hagiwara, T. Nohira, *J. Phys. Chem. C*, 2017, **121**, 18450.

[27]. J. Evans, C. A. Vincent, P. G. Bruce, *Polymer*, 1987, **28**, 2324.

[28]. S. Ferrari, E. Quartarone, P. Mustarelli, A. Magistris, S. Protti, S. Lazzaroni, M. Fagnoni, A. Albini, *J. Power Sources*, 2009, **194**, 45.

[29]. E. Peled, *J. Electrochem. Soc.*, 1979, **126**, 2047.

[30]. P. C. Howlett, D. R. MacFarlane, A. F. Hollenkamp, *Electrochem. Solid State Lett.*, 2004, **7**, A97.

Table of contents

A concentrated lithium salt electrolyte utilising the diethylpyrrolidinium cation and bis(fluorosulfonyl)imide anion shows high ionic conductivity and good Li electrochemistry